Accepted Manuscript

A comparative analysis of *corpora allata-corpora cardiaca* microRNA repertories revealed significant changes during mosquito metamorphosis

Marcela Nouzova, Kayvan Etebari, Fernando G. Noriega, Sassan Asgari

PII: S0965-1748(18)30088-2

DOI: 10.1016/j.ibmb.2018.03.007

Reference: IB 3044

To appear in: *Insect Biochemistry and Molecular Biology*

Received Date: 24 February 2018

Revised Date: 21 March 2018

Accepted Date: 22 March 2018

Please cite this article as: Nouzova, M., Etebari, K., Noriega, F.G., Asgari, S., A comparative analysis of *corpora allata-corpora cardiaca* microRNA repertories revealed significant changes during mosquito metamorphosis, *Insect Biochemistry and Molecular Biology* (2018), doi: 10.1016/j.ibmb.2018.03.007.

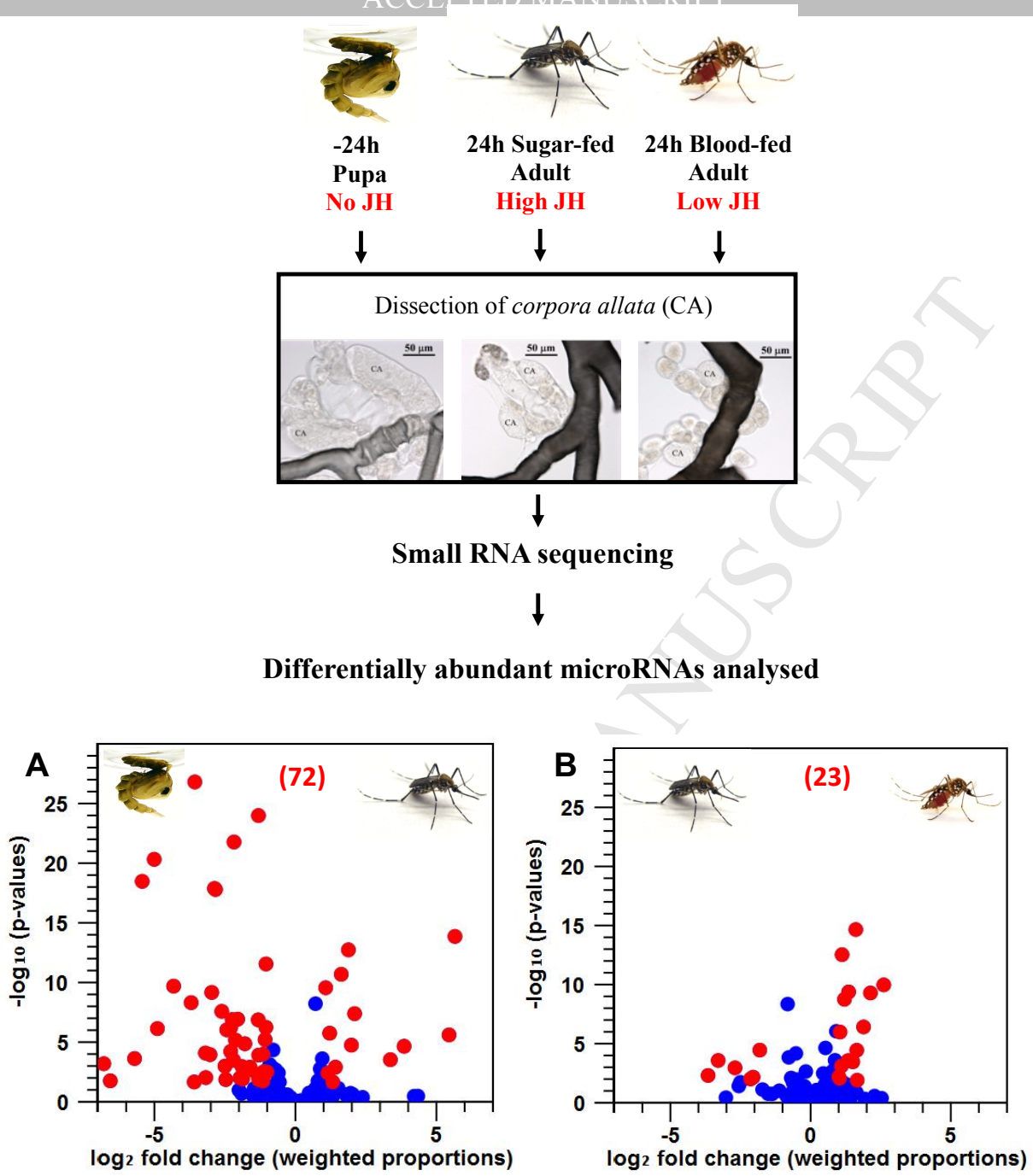

A comparative analysis of *corpora allata-corpora cardiaca* microRNA repertories revealed significant changes during mosquito metamorphosis

Marcela Nouzova[1#], Kayvan Etebari[2#], Fernando G. Noriega[1,3*] and Sassan Asgari[2*]

[1]Department of Biological Sciences, Florida International University, Miami, FL, 33199, USA.

[2]Australian Infectious Disease Centre, School of Biological Sciences, The University of Queensland, Brisbane, Australia

[3]Biomolecular Science Institute, Florida International University, Miami, FL, 33199, USA.

Running title: microRNA changes in mosquito corpora allata

[#]These two authors contributed equally to the work

*Corresponding author: s.asgari@uq.edu.au

*Corresponding author: noriegaf@fiu.edu

Abstract

The *corpora allata* (CA) are a pair of endocrine glands with neural connections to the brain and close association with another neuroendocrine organ, the *corpora cardiaca* (CC). The CA from adult female *Aedes aegypti* mosquitoes synthesizes fluctuating levels of juvenile hormone (JH), which have been linked to the ovarian development and are influenced by nutritional signals. In this study, we investigated the potential involvement of microRNAs (miRNAs), a type of small non-coding RNAs, in the regulation of gene expression in CA-CC complexes during mosquito reproductive development, at stages with distinct JH biosynthesis patterns. We analyzed the miRNA repertoires expressed in the CA-CC of pupae, sugar-fed and blood-fed female *Ae. aegypti*. In total, 156 mature miRNAs were detected in the CA-CC, with 84 displaying significant differences in expression among the three CA-CC developmental stages. There were more miRNAs that were expressed in pupae, and decreased or were absent after adult emergence, when compared with changes between CA-CC of sugar and blood-fed females. Analysis of the genes identified as potential targets for the CA-CC miRNA repertoires classified them into the broad categories of metabolism, information storage and processing, and cellular processes and signaling; with genes involved in cellular processes and signaling representing the largest portion. Among them, the signal-transduction mechanisms and intracellular trafficking, secretion and vesicular transport contained almost 55% of the genes' targets. A substantial number of miRNAs were differentially abundant in the three libraries, and those changes were much more notable when pupae and adult libraries were compared. We detected putative binding sites for some of the most abundant miRNAs on genes encoding JH biosynthetic enzymes and CC neuropeptides. These studies should help us to gain a better understanding of the regulation of CA-CC activity mediated by miRNAs during major developmental stages in mosquitoes.

Keywords: *Aedes aegypti*; copora allata; microRNA; metamorphosis; juvenile hormone

Introduction

Juvenile hormone (JH) is a key regulator of development and reproduction in insects (Goodman and Cusson, 2012). JH delays metamorphosis until *Aedes aegypti* mosquito larvae have attained an appropriate stage and size. At that point, a drop in JH titer permits a metamorphic molt. As the anti-metamorphic role of JH comes to an end, the late pupa becomes again "competent" to synthesize JH, which plays an essential role orchestrating reproductive maturation (Zhu and Noriega, 2016). JH is biosynthesized *de novo* by the *corpora allata* (CA), a pair of endocrine glands connected to the brain, and in close association with another neuroendocrine organ, the *corpora cardiaca* (CC) (Tobe and Stay, 1985). In mosquito larvae, the CA and CC, along with a third endocrine gland, the prothoracic gland (PG), are fused into the "gland complex" (GC) (Burgess and Rempel, 1966), analogous to the ring gland of *Drosophila*. The size, shape, and composition of the GC changes as the pupa transforms into an adult (Burgess and Rempel, 1966). Adult female mosquitoes show dynamic changes in JH synthesis, which have been related to their reproductive physiology; the CA is very active in sugar-fed females, however JH synthesis dramatically decreases after blood-feeding (Noriega, 2004; Rivera-Perez et al., 2014). The CC of adult mosquitoes is a neurohemal storage area fused around the aorta where peptide hormones produced in brain neurosecretory cells are released into the hemolymph (Clements et al., 1985; Meola and Lea, 1972). In addition, a posterior glandular part of the CC contains a group of neurosecretory cells (X cells), and axons from these cells extend to the CA. A critical CC product is adipokinetic hormone (AKH), a polypeptide that mobilizes stored macromolecular energy reserves to sustain energy-consuming activities, such as flight (van der Horst and Rodenburg, 2010).

MicroRNAs (miRNAs) are small non-coding RNAs that are generated in almost all eukaryotes and by viruses. The main function of miRNAs is regulation of gene expression at the post-transcriptional level, adding a new layer of control to the complex pathways that exists in cells. In many instances, miRNAs are essential for target tuning and optimal expression levels of genes (Bartel, 2004), having pleiotropic

roles by regulating transcripts of target genes at different times and locations during development (Chawla and Sokol, 2011). In insects, miRNAs are involved in the regulation of numerous biological processes, including development, reproduction, metamorphosis and responses to immune challenges (reviewed in Asgari, 2013; Belles, 2017; Lucas et al., 2013). In *Ae. aegypti*, studies of transcriptome-wide miRNA and target dynamics in the fat body during the gonadotrophic cycle suggested that miRNAs broadly regulate metabolic processes, in particular lipid transport and metabolism (Zhang et al., 2017). Specific miRNAs have been associated with the regulation of particular physiological processes in *Ae*. *aegypti*. Loss of miR-275 resulted in severe defects linked to inability to digest blood, excrete excessive fluids, and properly develop eggs (Bryant et al., 2010). In addition, miR-1174 targets serine hydroxymethyltransferase (SHMT) in the gut, and depletion of this miRNA resulted in severe defects in sugar absorption and blood intake (Liu et al., 2014). miR-1890 targets the juvenile hormone-regulated serine protease JHA15 in the female gut (Lucas et al., 2015b), while miR-8 targets the Wingless signaling pathway in the female fat body, critical for the proper secretion of lipophorin and vitellogenin, and subsequent accumulation of these yolk protein precursors by developing oocytes (Lucas et al., 2015a).

In this study, we analyzed the miRNA repertoires expressed in the GC of pupae, and CA-CC complexes of sugar-fed and blood-fed female *Ae. aegypti*. In total, 156 mature miRNAs were detected in the GC, with 84 displaying significant differences in abundance among the three developmental stages. Notably, the changes in the miRNA repertoire in the GC in the pupa-adult transition have completely different characteristics compared with the changes from sugar-fed to blood-fed mosquitoes.

Materials and Methods

Insects, tissue dissection and RNA extraction

Ae. aegypti of the Rockefeller strain were reared at 28 °C and 80% humidity as previously described (Rivera-Perez et al., 2014). Adult mosquitoes were offered a cotton pad soaked in a 3% sucrose solution. Four-day-old female mosquitoes were fed pig blood equilibrated to 37 °C, and ATP was added to the blood meal to a final concentration of 1 mM immediately before use as previously described (Rivera-Perez et al., 2014).

Corpora allata-corpora cardiaca complexes (CA-CC) were dissected from three different developmental stages of *Ae. aegypti* females; pupae 24h before adult emergence (-24h pupae), adult 24h after emergence fed 3% sugar (24h sugar-fed) and 4-day-old adults, blood-fed and collected 24h after blood feeding (24h blood-fed). Total RNA was extracted from 50 CAs from each developmental stage in triplicate using Norgen Biotek's total RNA purification kit. Total RNA was treated with DNase I according to Norgen Biotek's instructions.

Small RNA libraries preparation and sequencing

The small RNA libraries were generated using the Illumina Truseq™ Small RNA Preparation kit according to Illumina's TruSeq™ Small RNA Sample Preparation Guide and sequenced at LC Sciences facility (Texas, USA).

Revision of *Aedes aegypti* miRNA repertoire

The quality of raw data from each library was controlled using CLC Genomic Workbench version 7.5.1. Raw data were stripped of adapters and reads with quality score above 0.05 and less than 2 ambiguous nucleotides were retained. Reads without 3' adapters and reads with less than 16 nt were discarded from the libraries. Clean data were considered as "mappable reads" for further analysis. Tab separated files with the read sequences and their counts were used as input files for novel and homologous miRNA analysis using sRNAtoolbox (Rueda et al., 2015). Although sRNAtoolbox is a powerful tool for novel miRNA identification, all predicted miRNAs were individually inspected for their pre-miRNA secondary structure, mature miRNA position on the stem loop, and their abundance in

our libraries. We also double-checked their possible similarity with other RNA sequences (such as tRNA and rRNA) in Rfam. In addition, we examined all potential novel *Ae. aegypti* miRNAs, reported in previous publications (Akbari et al., 2013; Hu et al., 2015; Kozomara and Griffiths-Jones, 2014; Miesen et al., 2016; Zhang et al., 2017), and retained only highly confident miRNAs.

Ae. aegypti miRNAs were reannotated because several new RNA-Seq data, including this study, have become available since the initial deposition of *Ae. aegypti* miRNAs in miRBase. For this reannotation, stem loop secondary structures were predicted by a minimum free energy (MFE) approach using CLC Genomic Workbench (Zhuker, 1989). We used our current small RNA libraries, as well as previously produced libraries (SRP111336) (Lee et al., 2017), to reconsider the current *Ae. aegypti* miRNA annotation. The small RNA reads were mapped against known pre-miRNAs, and mapped reads with maximum counts in each arm were considered as "revised 5p or 3p miRNAs". To identify the most abundant isomiRs for each miRNA, we allowed matches to extend to maximum five additional nucleotides in both 5' and 3' ends of canonical sequences. We also removed those *Ae. aegypti* miRNAs whose majority of reads mapped to other parts of pre-miRNA sequences (including terminal loop), instead of 5p or 3p mature miRNAs. In addition, we discarded aae-miRNAs with less than 10 supportive reads (in at least 50% of the examined libraries) or unsuitable secondary structure (asymmetrical stem loop, and MFE above -19 Kcal/mol).

Small RNA data analysis and miRNA profiling

We used the small RNA tools available in CLC Genomic Workbench to extract and count unique small RNA reads with a minimum of five sampling count. All the revised 205 mature miRNAs were used as reference for miRNA profiling in this project. We allowed isomiRs with 5 nt variants to be detected in up and downstream of annotated mature miRNAs with maximum two mismatches in the aligned region.

We produced the miRNA profile for each library, and then all three biological replicates for each sample were used to set up a multi-group comparison experiment to measure miRNAs differential expression among pupa, sugar-fed and blood-fed adult samples. The expression values or mature miRNA copy numbers were normalized by their total read counts per million. This normalization method was applied to all data sets to calculate effective sizes of the libraries, which are then used as part of the per-sample normalization (Robinson and Oshlack, 2010).

Target identification

The latest assembly of the *Ae. aegypti* genome (GCF_000004015.4) was used as a reference. It contained 17,350 annotated genes in 4,757 scaffolds. We used three different algorithms including RNA22 (Miranda et al., 2006), miRanda (Enright et al., 2003) and RNAhybrid (Krueger and Rehmsmeier, 2006) to predict potential miRNA binding sites in all *Ae. aegypti* genes using their default parameters unless indicated. If partial mRNAs did not have a complete annotation, such as clear 5'UTR, ORF and 3'UTR, the region before the ORF start codon (300 bp) and after the stop codon (500 bp) for each mRNA were considered as 5'UTR and 3' UTR, respectively.

RNAhybrid is a tool for finding the normalized minimum free energy of hybridization for miRNAs and their mRNA target genes. The small RNA sequence is hybridized to the best fitting part of the mRNA. We did not allow G:U pairing in the seed region (nucleotide 2-8), and forced miRNA-target duplexes to have a helix in this region. Maximum 5 nt were approved as unpaired nucleotides in either side of an internal loop. miRanda also considers matching along the entire miRNA sequence, but we ran the program in the strict mode, which demands a strict 5' seed pairing. It takes the seed region into account by adding more value to matches in the seed region. The RNA22 version 2 is a pattern based target prediction program, which first searches for reverse complement sites of patterns within given mRNA sequence, and identifies the hot spots. In the next step, the algorithm searches for miRNAs that are likely to bind to these sites. We allowed a maximum of one mismatch in the seed region, and a

minimum of 12 nt matches in the entire binding site. We set the sensitivity and specificity thresholds on 63% and 61%, respectively. To increase the level of confidence, we preferred those binding sites that were predicted by all the three algorithms for further analysis.

Annotation of KOG for *Ae. aegypti* genes was done as described in Ribeiro et al. (Ribeiro et al., 2007).

miRNA-specific reverse transcription quantitative PCR (RT-qPCR)

To validate the RNA-Seq data, we selected nine miRNA that were abundant and differentially expressed in the three libraries, and assessed their changes using RT-qPCR. The CA-CC were dissected from female mosquitoes at pupal and adult stages (sugar-fed or blood-fed) as described above. For each developmental stage, three biological replicates were prepared, each containing pools of CA-CC from 30 mosquitoes. RNA was extracted from the samples using Norgen Biotek's total RNA purification kit and treated with DNase I as described in the manufacturer's instructions. First strand cDNA was synthesized with a miScript II RT kit following the manufacturer's instructions (Qiagen). The abundances of miRNAs were measured in a 7500 real-time PCR system (Applied Biosystems), using QuantiTech SYBR green mix and a Qiagen universal reverse primer, together with custom forward primers, which were the mature miRNA sequences. Melt curve analysis was performed after each run to ensure the specificity of amplification. All reactions were performed in three biological replicates each with three technical replicates, and a template-free control was included in all batches. A U6 primer was used as a reference for normalization of data. Sequences of all primers are listed in Table S4.

Availability of data

All sequence data were deposited in the GenBank under Gene Expression Omnibus accession GSE99498.

Results and Discussion

***Aedes aegypti corpora allata-corpora cardiaca* miRNA repertoire**

miRNAs can regulate developmental transitions and reproductive maturation processes through cell-type-specific, as well as stage-specific expression patterns. Comparing miRNA profiles between different stages of development has facilitated the identification of miRNAs involved in controlling these types of progressions. Previous studies in insects suggested the relevance of making organ-specific libraries when the aim is to obtain robust conclusions on miRNA roles in particular tissues (Cristino et al., 2010). We studied the dynamics of CA-CC miRNAs in female *Ae. aegypti* during pupa-adult transition, as well as during reproductive maturation before and after blood feeding. Gland complexes were carefully dissected from three very different stages that have distinct JH biosynthesis rates; namely, the early pupa (non-detectable JH synthesis), the sugar-fed female (high JH synthesis), and the blood-fed female (very low JH synthesis) (Zhu and Noriega, 2016) (Fig. 1). Small RNA libraries were constructed with three biological replicates at each time point, and sequenced to generate 10-28 million clean reads, with over 95% of them mapped to the mosquito genome (Table 1). Small RNA libraries were sequenced and data were analyzed following the procedures described as a flow chart in Fig. 1. Briefly, data analysis and interpretation included data processing, data quality assessment, data normalization and determination of differential abundances of miRNAs.

Although 101 precursors and 124 mature *Ae. aegypti* miRNAs were annotated in miRBase (aae-miR) (Li et al., 2009), there was a need to extend and correct the current miRNA repertoire of this species, according to its latest genome assembly, as well as additional available small RNA sequence data for high confidence miRNAs, with the correct 5p and 3p arm features. Therefore, the latest list of aae-miRs reported in miRBase was downloaded, and their pre-miRNA secondary structures were assessed to confirm the location of mature miRNA position on each arm. In addition, novel miRNAs were identified using the approach described in the methods section. In total, we annotated 121 pre-miRNAs, with 101 of them already present in miRBase and 20 novel or already reported as novel in previous studies (Akbari et al., 2013; Bartel, 2009; Hu et al., 2015; Kozomara and Griffiths-Jones, 2014; Zhang

et al., 2017) (Table S1). These pre-miRNAs produced 234 mature miRNAs, with 196 already described in miRBase and 38 novel (Table S1). After excluding duplicated mature miRNAs, 205 were unique.

A generally accepted hypothesis suggests that most miRNAs only 'fine tune' the expression of the majority of their targets, with just a small number of target genes experiencing a large change in mRNA or protein abundance (Bartel, 2009). The relationship between the abundance of specific miRNAs and the importance of their potential regulatory roles is intricate. Although miRNA levels eventually define the extent of gene repression, there is a complex stoichiometric relationship between factors such as miRNAs and target abundance, target-site spacing, and affinity requirements of different endogenous competitive targets (Denzler et al., 2016). In other words, in a particular tissue and developmental stage, not always the most abundant miRNAs are those playing critical roles in gene regulation.

miRNA studies in different species of insects have revealed differences, as well as similarities among the most abundant miRNAs expressed. Frequently, the most abundant miRNAs changed with each analyzed tissue, and often also changed with the developmental stage (Cristino et al., 2010). In the locust *Locusta migratoria*, miR-1, miR-275, miR-276 and miR-8 predominated (Wei et al., 2009). In the silkworm *Bombyx mori*, miR-1, miR-8, miR-276 and miR-263 were the most abundant (Jagadeeswaran et al., 2010); with miRNAs showing diverse and dynamic expression patterns in multiple silkworm tissues (Liu et al., 2010). These strong varying spatiotemporal patterns of miRNA expression in the silkworm from the larval to pupal stages included changes in expression from the two arms of a particular precursor miRNA (3' or 5' arms), as well as sense and antisense transcripts (Liu et al., 2010); suggesting a diverse miRNA repertoire playing roles in tissue-specific remodeling during metamorphosis.

Previous studies have identified miR-184 as the most abundant miRNA in *Ae. aegypti* (Li et al., 2009; Mayoral et al., 2014), as well as in other Culicinae, such as *Aedes albopictus* and *Culex*

quinquefasciatus (Skalsky et al., 2010). Studies in *Anopheles gambiae* mosquitoes identified miR-10, miR-184, miR-281 and bantam as the most abundantly expressed miRNAs in adult females (Lampe and Levashina, 2018). In *An. gambiae*, the group of most abundant miRNAs changed before and after blood-feeding, and some of them dominated the repertoire only in specific tissues; for instance miR-281 in the midgut, miR-10 and miR-306 in the ovary and miR-8 and miR-276 in the head and fat body (Lampe and Levashina, 2018).

We evaluated the most abundant miRNAs in each of the libraries. In total, 156 mature miRNAs were detected in the CA-CC, with 84 displaying significant differences in abundance among the three CA-CC developmental stages. Fig. S1 shows the clustering of the nine libraries based on the normalized abundance of all miRNAs detected in the CA-CC, with the specific replicates clustering together. The most abundant 20 miRNAs expressed in each of the stages are presented in Fig. 2A. As previously described for *Ae. aegypti* whole body (Mayoral et al., 2014), the most abundant miRNA in all the libraries was miR-184-3p, representing 48% of the reads from CA-CC of sugar-fed and 40% of the reads from CA-CC of blood-fed females, but only 16% of the reads from pupae CA-CC. The functional role of miR-184 has mainly been established in *Drosophila*, in which it has been implicated in peripheral nervous system development (Peng et al., 2015), female gremlin development (Iovino et al., 2009), ovary morphogenesis (Yang et al., 2016), and motility (Peng et al., 2015). In *Ae. aegypti*, the abundance of miR-184-3p declines in the fat body in blood-fed mosquitoes as compared to non-blood fed mosquitoes (Zhang et al., 2017). We also observed reductions in miR-184-3p when comparing CA-CC from blood-fed and sugar-fed mosquitoes (Fig. 2A). With FOXL, a transcription factor that is involved in egg development, determined as a potential target of miR-184-3p. It has been proposed that the interaction of the miRNA and its target may contribute to homeostasis of FOXL, and sustain egg development (Zhang et al., 2017).

A Venn diagram shows the number of those 20 more abundant miRNAs that are shared or are unique for each library (Fig. 2B). A number of miRNAs were differentially expressed among the three developmental stages, and those changes were much more notable when pupae and adult libraries were compared. In our studies, the miRNA repertoire of pupae CA-CC was more diverse and heterogeneous than those of the adult female CA-CC (Fig. 3), with three additional miRNAs, miR-8-3p, miR-100-5p and miR-276-1-3p, representing each 11-12% of the reads. The volcano plots also revealed that there were more miRNAs that were expressed in pupae, and decreased or were absent after adult emergence, when compared with changes between CA-CC of sugar and blood-fed females (Fig. 4 and Tables S2a and S2b).

Hierarchical clustering analysis of the miRNAs expressed in the three different developmental stages revealed five major groups representing distinct expression patterns (Fig. 5). Some miRNAs were pupa specific (group II) and some were adult specific (group IV and V); with miRNAs that were either expressed only in libraries from blood-fed females (group IV) or were absent only after a blood-meal (group I). Finally, there were some miRNAs present only in the CA-CC that show diminished JH group synthesis, such as those from pupae and blood-fed females (group III). We speculate that some miRNAs from group III could be involved in the regulation of JH synthesis, since their expression pattern negatively correlates with changes in JH synthesis levels, which are low in pupae, high in sugar-fed and low in blood-fed mosquitoes. On the other hand, miRNAs from group II and V might play roles in the developmental changes that occur in the gland during metamorphosis.

To validate the RNA-Seq data, the CA-CC from the three developmental stages (pupa, sugar-fed and blood-fed female mosquitoes) were independently dissected and subjected to RNA extraction and mature miRNA quantification using miRNA-specific RT-qPCR. For this validation, nine miRNAs were selected. Comparison of the results between RNA-Seq and RT-qPCR revealed consistency between the two methods, with all the nine miRNAs analyzed showing similar trends (Fig. 6).

279 It has been described that miRNAs can provide an effective means by which to set thresholds and limit
280 noise-induced errors to ensure robustness during developmental transitions (Cohen et al., 2006). The
281 miRNA changes observed in our study might reflect developmental modifications of the GC; as the GC
282 changes in size, shape, and composition when the pupa transforms into an adult (Burgess and Rempel,
283 1966). The most important of these changes is the prothoracic gland degeneration, a programmed cell
284 death process by apoptosis and autophagy (Romer and Martau, 1998). miRNAs contribute significantly
285 to autophagy, mediating acute responses to starvation, hypoxia and other types of stress (Zhai et al.,
286 2013). Several of the miRNAs that are abundant in the CA-CC libraries have been previously
287 implicated in autophagy control, including miR-184 (Liu et al., 2015), miR-100 (Ge et al., 2014), miR-
288 34 and miR-30 (Zhai et al., 2013). In summary, some of the pupa-specific miRNAs might be involved
289 in the regulation of PG degeneration or additional metamorphic changes in the GC. Some might play a
290 role in inhibiting JH synthesis, since PG degeneration is effectively prevented by the presence of JH
291 (Mane-Padros et al., 2010).

292 **Targets for the *corpora allata-corpora cardiaca* miRNA repertoires**

293 Bioinformatics approaches were used to determine potential targets for miRNAs. *In silico* methods
294 included the search for (1) miRNA binding sites on specific genes of interest, such as those encoding
295 JH biosynthetic enzymes and CC neuropeptides, and (2) miRNA target genes using the Eukaryotic
296 Clusters of Orthologous Groups analysis (KOG), an approach employed to classify proteins into
297 functional categories on the basis of orthology (Tatusov et al., 2000).

298 We used three different algorithms to predict potential miRNA binding sites in the 13 *Ae. aegypti* genes
299 encoding JH biosynthetic enzymes (Rivera-Perez et al., 2014). Four of the enzymes had miRNA
300 binding sites that were predicted by all three algorithms, and five of these miRNAs were among the 20
301 most abundant miRNAs detected in at least one of the three CA-CC libraries; with miR-31-5p targeting
302 *3-hydroxy-3-methylglutaryl-coenzyme A reductase* (*HMGR*), bantam-3p targeting

303 *diphosphomevalonate decarboxylase* (*PP-MevD*), miR-34-5p targeting *PP-MevD* and *aldehyde*
304 *dehydrogenase* (*ALDH*), and miR-9a-5p targeting *farnesyl-pyrophosphate synthase* (*FPPS*) (Table S3).
305 Interestingly, miR-34-5p, which was abundant only in the CA-CC of blood-fed females, targets *ALDH*.
306 It has been previously described that the low catalytic activity of ALDH limits JH synthesis and plays a
307 key role in the regulation of CA activity in blood-fed *Ae. aegypti* females (Rivera-Perez et al., 2013).
308 We used the same three algorithms to predict potential miRNA binding sites in four genes encoding
309 neuropeptides synthesized in the CC, namely adipokinetic hormone 1 (AKH1), AKH2, corazonin and
310 crustacean cardioactive peptide (CCAP) (Predel et al., 2010). Two programs predicted the same
311 binding sites for miR-305-5p and miR-980-5p in *corazonin*, as well as binding sites for miR-285-3p
312 and miR-210-3p in *AKH2*. The algorithm RNAhybrid predicted additional binding sites for some of the
313 most abundant 20 miRNAs detected in *Ae. aegypti* CA-CC, which were not confirmed by the other two
314 programs. This group included binding sites for miR-31-5p, miR-8-5p, miR-34-5p, miR-92b-3p and
315 miR-305-5p in *AKH1*, binding sites for miR-34-5p and miR-998-3p in *AKH2*, binding sites for miR-
316 125-5p, miR-34-5p, let-7-5p, miR-184-3p and miR-92b-3p in *CCAP*, as well as binding sites for miR-
317 275-3p and miR-305-5p in *corazonin* (Table S3). The potential roles of any of these miRNAs in the
318 regulation of the expression of JH biosynthetic enzymes or CC neuropeptides will require additional
319 functional experiments.
320 A KOG analysis of the genes identified as potential targets for the CA-CC miRNA repertoires
321 classified them into the broad categories of metabolism, information storage and processing, and
322 cellular processes and signaling; with genes involved in cellular processes and signaling representing
323 the largest portion. Among them, the signal-transduction mechanisms and intracellular trafficking,
324 secretion and vesicular transport contained almost 55% of the target genes. When a similar KOG
325 analysis was performed using the whole *Ae. aegypti* transcriptome, the results were very similar,

suggesting that this type of analysis was unable to identify a specific set of genes that are targeted by the differentially expressed CA-CC miRNA set (Fig. S2).

Most miRNAs are predicted to have hundreds of potential target genes, and often these target sites are conserved in evolution, providing some confidence that they are indeed functional. Yet, in several cases, a miRNA, as assessed by its mutant phenotype, has a significant effect on one or a few of the predicted targets (Bushati and Cohen, 2007). Several miRNAs have been previously described as modulators of hormonal pathways in insects. Insulin production and secretion, as well as cellular responsiveness to insulin, are subject to regulation by miRNAs. In *Drosophila*, miR-14 acts in the insulin-producing neurosecretory cells in the adult *Drosophila* brain to control metabolism; miR-14 acts in these brain cells through its direct target gene, *sugarbabe*, which encodes a predicted zinc finger protein that regulates insulin gene expression in the neurosecretory cells. Regulation of *sugarbabe* levels by nutrients and by miR-14 come together to allow the fly to manage resource mobilization in a nutritionally variable environment (Varghese et al., 2011). In *Drosophila*, miR-14 also plays a key role in modulating the positive auto regulatory loop by which ecdysone sensitizes its own signaling pathway. miR-14 modulates this loop by limiting expression of its target, the ecdysone receptor (EcR), while ecdysone signaling, via EcR, down-regulates miR-14 (Varghese and Cohen, 2007). A mutual repression between miR-34 and steroid hormone signaling was also described in *Drosophila*; ecdysone strongly inhibits miR-34 expression via transcriptional repression assisted by a number of transcription factors, including the ecdysone receptor and the Broad Complex, two key mediators of the ecdysone signaling cascade (Xiong et al., 2016). miR-281 regulates the expression of EcR in *B. mori* (Jiang et al., 2013), suggesting a widespread role of miRNAs in the regulation of ecdysteroid signaling.

Additional miRNAs play critical roles controlling metamorphosis, such as let-7 in silkworms (Ling et al., 2014) and cockroaches (Rubio and Belles, 2013). During the transition from nymph to adult in

cockroaches, miR-2 scavenges *Krüppel homolog 1* (*Kr-h1*) transcripts, a juvenile hormone-dependent transcription factor that represses metamorphosis (Lozano et al., 2015).

Less is known about the role of miRNAs on the control of CA activity and JH synthesis. A recent study described honey bee queen and drone caste-specific miRNAs and transcriptomic changes. This occurs during a critical time of larval development when JH titers are significantly higher in queen larvae than drones. Accordingly, there were significant decreases in the transcripts of many JH biosynthetic enzymes in drones, in particular of JH acid methyltransferase (JHAMT) and epoxidase, the last two critical enzymes in the pathway. In addition, there were as well substantial changes in the expression of many miRNAs when queens and drones larvae were compared; but no genes within the JH pathway were predicted to be a target of any of these fluctuating miRNAs (Ashby et al., 2016). On the contrary, a recent study in *Drosophila* described that loss-of-function of miRNA bantam increased *JHAMT* expression, while overexpression of bantam repressed *JHAMT* expression and resulted in pupal lethality (Qu et al., 2017). The male genital organs of the pupae were malformed, and exogenous sesquiterpenoid application partially rescued the genital deformities. The role of bantam on the regulation of sesquiterpenoid biosynthesis was validated by transcriptomic, qPCR, and hormone titer (JHB3 and JH III) analyses (Qu et al., 2017).

The CA-CC-specific miRNA repertoires identified in this study offer groundwork for forthcoming functional studies. In the future, selected miRNA mimics can be used to transfect the CA in *vitro*, and assess the effect on JH synthesis (Li et al., 2003). Other potential functional studies include the analysis of phenotypic changes when antagomirs are used to silence endogenous miRNAs (Schoniger and Arenz, 2013). This approach has been successfully employed to confirm the role of miR-8 in regulating mosquito reproductive processes by the fat body (Lucas et al., 2015a). Additional approaches that have been successfully employed to characterize miRNA functions in insects include silencing the expression of Dicer-1, the ribonuclease that produces mature miRNAs from miRNA precursors. Dicer-

1 deletion was used to validate the role of miR-2 in controlling the JH signaling pathway during metamorphosis in cockroaches (Lozano et al., 2015). Alternatively, cross-linking and immunoprecipitation of the core miRNA binding partner, Argonaute (AGO1 CLIP-Seq), has been successfully used to identify miRNA targets in the fat body of *Ae. aegypti* (Zhang et al., 2016). Similar approaches could be used to explore miRNA targets in the CA-CC.

In summary, our studies revealed that there are remarkable changes in the miRNA repertoires among the three stages of CA-CC studied. The changes are more profound between pupa and adult CA-CC, and that is in agreement with the idea that miRNAs play a major role in metamorphosis. There is a chance that the JH biosynthesis genes are not direct targets of miRNAs, and most likely the targets are signaling genes. Functional studies with selected miRNAs are currently designed to test this hypothesis.

Acknowledgements

This project was funded by a National Institute of Health grant (NIH-2015-2020) to FGN and an Australian Research Council grant (DP150101782) to SA.

References

Akbari, O., Antoshechkin, I., Amrhein, H., Williams, B., Diloreto, R., Sandler, J., Hay, B., 2013. The developmental transcriptome of the mosquito *Aedes aegypti*, an invasive species and major arbovirus vector. G3 3, 1493-1509.

Asgari, S., 2013. MicroRNA functions in insects. Insect Biochem Mol Biol 43, 388-397.

Ashby, R., Foret, S., Searle, I., Maleszka, R., 2016. MicroRNAs in honey bee caste determination. Sci Rep 6, 18794.

Bartel, D.P., 2004. MicroRNAs: Genomics, biogenesis, mechanism, and function. Cell 116, 281–297.

Bartel, D.P., 2009. MicroRNAs: target recognition and regulatory functions. Cell 23, 215-233.

Belles, X., 2017. MicroRNAs and the evolution of insect metamorphosis. Annu Rev Entomol 62, 111-125.

Bryant, B., Macdonad, W., Raikhel, A.S., 2010. microRNA miR-275 is indispensable for blood digestion and egg development in the mosquito *Aedes aegypti*. Proc Natl Acad Sci USA 107, 22391-22398.

Burgess, L., Rempel, J.G., 1966. The stomodaeal nervous system, the neurosecretory system, and the gland complex in *Aedes aegypti* (L.) (Diptera: Culicidae). Can J Zool 44, 731-765.

Bushati, N., Cohen, S.M., 2007. microRNA functions. Annu Rev Cell Dev Biol 23, 175-205.

Chawla, G., Sokol, N.S., 2011. MicroRNAs in *Drosophila* development. Int Rev Cell Mol Biol 286, 1-65.

406 Clements, A., Potters, S., Scales, M., 1985. The cardiacal neurosecretory system and associated organs
407 of an adult mosquito, *Aedes aegypti*. J Insect Physiol 31, 821-830.
408 Cohen, S.M., Brennecke, J., Stark, A., 2006. Denoising feedback loops by thresholding--a new role for
409 microRNAs. Genes Dev 20, 2769-2772.
410 Cristino, A.S., Tanaka, E.D., Rubio, M., Piulachs, M.D., Belles, X., 2010. Deep sequencing of organ-
411 and stage-specific microRNAs in the evolutionarily basal insect *Blattella germanica* (L.)
412 (Dictyoptera, Blattellidae). PLoS One 6, e19350.
413 Denzler, R., McGeary, S.E., Title, A.C., Agarwal, V., Bartel, D.P., Stoffel, M., 2016. Impact of
414 microRNA levels, target-site complementarity, and cooperativity on competing endogenous
415 RNA-regulated gene expression. Mol Cell 64, 565-579.
416 Enright, A.J., John, B., Gaul, U., Tuschl, T., Sander, C., Marks, D.S., 2003. MicroRNA targets in
417 *Drosophila*. Genome Biol 5, R1.
418 Ge, Y.Y., Shi, Q., Zheng, Z.Y., Gong, J., Zeng, C., Yang, J., Zhuang, S.M., 2014. MicroRNA-100
419 promotes the autophagy of hepatocellular carcinoma cells by inhibiting the expression of mTOR
420 and IGF-1R. Oncotarget 5, 6218-6228.
421 Goodman, W.G., Cusson, M., 2012. The juvenile hormones, in: Gilbert, L.I. (Ed.), Insect
422 endocrinology. Elsevier, pp. 310-365.
423 Hu, W., Criscione, F., Liang, S., Tu, Z., 2015. MicroRNAs of two medically important mosquito
424 species: *Aedes aegypti* and *Anopheles stephensi*. Insect Mol Biol 24, 240-252.
425 Iovino, N., Pane, A., Gaul, U., 2009. miR-184 has multiple roles in *Drosophila* female germline
426 development. Dev Cell 17, 123-133.
427 Jagadeeswaran, G., Zheng, Y., Sumathipala, N., Jiang, H., Arrese, E.L., Soulages, J.L., Zhang, W.,
428 Sunkar, R., 2010. Deep sequencing of small RNA libraries reveals dynamic regulation of
429 conserved and novel microRNAs and microRNA-stars during silkworm development. BMC
430 Genomics 11, 52.
431 Jiang, J., Ge, X., Li, Z., Wang, Y., Song, Q., Stanley, D.W., Tan, A., Huang, Y., 2013. MicroRNA-281
432 regulates the expression of ecdysone receptor (EcR) isoform B in the silkworm, *Bombyx mori*.
433 Insect Biochem Mol Biol 43, 692-700.
434 Kozomara, A., Griffiths-Jones, S., 2014. miRBase: annotating high confidence microRNAs using deep
435 sequencing data. Nucleic Acids Res 42, D68-D73.
436 Krueger, J., Rehmsmeier, M., 2006. RNAhybrid: microRNA target prediction easy, fast and flexible.
437 Nucleic Acids Res 34, W451-W454.
438 Lampe, L., Levashina, E.A., 2018. MicroRNA tissue atlas of the Malaria mosquito *Anopheles gambiae*.
439 G3 8, 185-193.
440 Lee, M., Etebari, K., Hall-Mendelin, S., van den Hurk, A.F., Hobson-Peters, J., Vatipally, S.,
441 Schnettler, E., Hall, R., Asgari, S., 2017. Understanding the role of microRNAs in the interaction
442 of *Aedes aegypti* mosquitoes with an insect-specific flavivirus. J Gen Virol 98, 892-1903.
443 Li, S., Mead, E.A., Liang, L., Tu, Z., 2009. Direct sequencing and expression analysis of a large
444 number of miRNAs in *Aedes aegypti* and a multi-species survey of novel mosquito miRNAs.
445 BMC Genomics 10, 581.
446 Li, Y., Hernandez-Martinez, S., Unnithan, G.C., Feyereisen, R., Noriega, F.G., 2003. Activity of the
447 corpora allata of adult female *Aedes aegypti*: effects of mating and feeding. Insect Biochem Mol
448 Biol 33, 1307-1315.
449 Ling, L., Ge, X., Li, Z., Zeng, B., Xu, J., Aslam, A.F., Song, Q., Shang, P., Huang, Y., Tan, A., 2014.
450 MicroRNA Let-7 regulates molting and metamorphosis in the silkworm, *Bombyx mori*. Insect
451 Biochem Mol Biol 53, 13-21.
452 Liu, S., Gao, S., Zhang, D., Yin, J., Xiang, Z., Xia, Q., 2010. MicroRNAs show diverse and dynamic
453 expression patterns in multiple tissues of *Bombyx mori*. BMC Genomics 11, 85.

Liu, S., Lucas, K., Roy, S., Ha, J., Raikhel, A., 2014. Mosquito-specific microRNA-1174 targets serine hydroxymethyltransferase to control key functions in the gut. Proc Natl Acad Sci USA 111, 14460-14465.

Liu, X., Fu, B., Chen, D., Hong, Q., Cui, J., Li, J., Bai, X., Chen, X., 2015. miR-184 and miR-150 promote renal glomerular mesangial cell aging by targeting Rab1a and Rab31. Exp Cell Res 336, 192-203.

Lozano, J., Montanez, R., Belles, X., 2015. MiR-2 family regulates insect metamorphosis by controlling the juvenile hormone signaling pathway. Proc Natl Acad Sci U S A 112, 3740-3745.

Lucas, K., Myles, K., Raikhel, A., 2013. Small RNAs: a new frontier in mosquito biology. Trends Parasitol 29, 295-303.

Lucas, K., Roy, S., Ha, J., Gervaise, A., Kokoza, V., Raikhel, A., 2015a. MicroRNA-8 targets the Wingless signaling pathway in the female mosquito fat body to regulate reproductive processes. Proc Natl Acad Sci USA 112, 1440-1445.

Lucas, K.J., Zhao, B., Roy, S., Gervaise, A.L., Raikhel, A.S., 2015b. Mosquito-specific microRNA-1890 targets the juvenile hormone-regulated serine protease JHA15 in the female mosquito gut. RNA Biol 12, 1383-1390.

Mane-Padros, D., Cruz, J., Vilaplana, L., Nieva, C., Urena, E., Belles, X., Martin, D., 2010. The hormonal pathway controlling cell death during metamorphosis in a hemimetabolous insect. Dev Biol 346, 150-160.

Mayoral, J., Etebari, K., Hussain, M., Khromykh, A., Asgari, S., 2014. *Wolbachia* infection modifies the profile, shuttling and structure of microRNAs in a mosquito cell line. PLoS One 9, e96107.

Meola, S.M., Lea, A.O., 1972. The ultrastructure of the corpus cardiacum of *Aedes sollicitans* and the histology of the cerebral neurosecretory system of mosquitoes. Gen Comp Endocrinol 18, 210-234.

Miesen, P., Ivens, A., Buck, A., van Rij, R., 2016. Small RNA profiling in dengue virus 2-infected *Aedes* mosquito cells reveals viral piRNAs and novel host miRNAs. PLoS Negl Trop Dis 10, e0004452.

Miranda, K.C., Huynh, T., Tay, Y., Ang, Y.-S., Tam, W.-L., Thomson, A.M., Lim, B., Rigoutsos, I., 2006. A pattern-based method for the identification of microRNA binding sites and their corresponding heteroduplexes. Cell 126, 1203-1217.

Noriega, F.G., 2004. Nutritional regulation of JH synthesis: a mechanism to control reproductive maturation in mosquitoes? Insect Biochem Mol Biol 34, 687-693.

Peng, J., Wang, C., Wan, C., Zhang, D., Li, W., Li, P., Kong, Y., Yuan, L., 2015. miR-184 is Critical for the motility-related PNS development in *Drosophila*. Int J Dev Neurosci 46, 100-107.

Predel, R., Neupert, S., Garczynski, S.F., Crim, J.W., Brown, M.R., Russell, W.K., Kahnt, J., Russell, D.H., Nachman, R.J., 2010. Neuropeptidomics of the mosquito *Aedes aegypti*. J Proteome Res 9, 2006-2015.

Qu, Z., Bendena, W.G., Nong, W., Siggens, K.W., Noriega, F.G., Kai, Z.P., Zang, Y.Y., Koon, A.C., Chan, H.Y.E., Chan, T.F., Chu, K.H., Lam, H.M., Akam, M., Tobe, S.S., Lam Hui, J.H., 2017. MicroRNAs regulate the sesquiterpenoid hormonal pathway in *Drosophila* and other arthropods. Proc Biol Sci 284,

Ribeiro, J.M., Arca, B., Lombardo, F., Calvo, E., Phan, V.M., Chandra, P.K., Wikel, S.K., 2007. An annotated catalogue of salivary gland transcripts in the adult female mosquito, *Aedes aegypti*. BMC Genomics 8, 6.

Rivera-Perez, C., Nouzova, M., Clifton, M.E., Garcia, E.M., LeBlanc, E., Noriega, F.G., 2013. Aldehyde dehydrogenase 3 converts farnesal into farnesoic acid in the corpora allata of mosquitoes. Insect Biochem Mol Biol 43, 675-682.

Rivera-Perez, C., Nouzova, M., Lamboglia, I., Noriega, F.G., 2014. Metabolic analysis reveals changes in the mevalonate and juvenile hormone synthesis pathways linked to the mosquito reproductive physiology. Insect Biochem Mol Biol 51, 1-9.

Robinson, M., Oshlack, A., 2010. A scaling normalization method for differential expression analysis of RNA-seq data. Genome Biol 11, R25.

Romer, F., Martau, T., 1998. Degeneration of moulting glands in male crickets. J Insect Physiol 44, 981-989.

Rubio, M., Belles, X., 2013. Subtle roles of microRNAs let-7, miR-100 and miR-125 on wing morphogenesis in hemimetabolan metamorphosis. J Insect Physiol 59, 1089-1094.

Rueda, A., Barturen, G., Lebron, R., Gomez-Martin, C., Alganza, A., Oliver, J.L., Hackenberg, M., 2015. sRNAtoolbox: an integrated collection of small RNA research tools. Nucleic Acids Res 43, W467-W473.

Schoniger, C., Arenz, C., 2013. Perspectives in targeting miRNA function. Bioorg Med Chem 21, 6115-6118.

Skalsky, R., Vanlandingham, D.L., Scholle, F., Higgs, S., Cullen, B.R., 2010. Identification of microRNAs expressed in two mosquito vectors, *Aedes albopictus* and *Culex quinquefasciatus*. BMC Genomics 11, 119.

Tatusov, R.L., Galperin, M.Y., Natale, D.A., Koonin, E.V., 2000. The COG database: a tool for genome-scale analysis of protein functions and evolution. Nucleic Acids Res 28, 33-36.

Tobe, S.S., Stay, B., 1985. Structure and regulation of the corpus allatum, in: Berridge, M.J., Treherne, J.E., Wigglesworth, V.B. (Eds.), Advances in Insect Physiology. Elsevier, pp. 305-432.

van der Horst, D.J., Rodenburg, K.W., 2010. Locust flight activity as a model for hormonal regulation of lipid mobilization and transport. J Insect Physiol 56, 844-853.

Varghese, J., Cohen, S., 2007. microRNA miR-14 acts to modulate a positive autoregulatory loop controlling steroid hormone signaling in *Drosophila*. Genes Dev 21, 2277 - 2282.

Varghese, J., Lim, S.F., Cohen, S.M., 2011. *Drosophila* miR-14 regulates insulin production and metabolism through its target, *sugarbabe*. Genes Dev 24, 2748–2753.

Wei, Y., Chen, S., Yang, P., Ma, Z., Kang, L., 2009. Characterization and comparative profiling of the small RNA transcriptomes in two phases of locust. Genome Biol 10, R6.

Xiong, X.P., Kurthkoti, K., Chang, K.Y., Li, J.L., Ren, X., Ni, J.Q., Rana, T.M., Zhou, R., 2016. miR-34 modulates innate immunity and ecdysone signaling in *Drosophila*. PLoS Pathog 12, e1006034.

Yang, H., Li, M., Hu, X., Xin, T., Zhang, S., Zhao, G., Xuan, T., Li, M., 2016. MicroRNA-dependent roles of Drosha and Pasha in the *Drosophila* larval ovary morphogenesis. Dev Biol 416, 312-323.

Zhai, H., Fesler, A., Ju, J., 2013. MicroRNA: a third dimension in autophagy. Cell Cycle 12, 246-250.

Zhang, X., Aksoy, E., Girke, T., Raikhel, A.S., Karginov, F.V., 2017. Transcriptome-wide microRNA and target dynamics in the fat body during the gonadotrophic cycle of *Aedes aegypti*. Proc Natl Acad Sci U S A 114, E1895-E1903.

Zhang, Y., Zhao, B., Roy, S., Saha, T.T., Kokoza, V.A., Li, M., Raikhel, A.S., 2016. microRNA-309 targets the Homeobox gene SIX4 and controls ovarian development in the mosquito *Aedes aegypti*. Proc Natl Acad Sci U S A 113, E4828–E4836.

Zhu, J., Noriega, F., 2016. The role of juvenile hormone in mosquito development and reproduction, in: Raikhel, A.S. (Ed.), Advances in Insect Physiology. Elsevier, pp. 93-113.

Zhuker, M., 1989. The use of dynamic programming algorithms in RNA secondary structure prediction, in: Waterman, M. (Ed.), Mathematical methods for DNA sequences. CRC Press, Boca Raton, FL, pp. 159-184.

548 **Figure legends**

549 **Fig. 1: Experimental flow chart**: Small RNA libraries were sequenced and data were analyzed
550 following the procedures described in the flow chart. Data analysis and interpretation included
551 data processing, data quality assessment, data normalization and determination of differential
552 abundances of miRNAs.

553 **Fig. 2: The most abundant 20 miRNAs expressed in each developmental stage:** (A) The
554 most abundant 20 miRNAs expressed in each of the stages. miRNA expression is shown as
555 normalized reads per million. (B) Venn diagram showing the number of those 20 more abundant
556 miRNAs that are unique for each library.

557 **Fig. 3: Doughnut diagrams of proportions of the first 20 most abundant miRNAs in each**
558 **developmental stage.** The three circles within the diagram represent biological replicates. -24 h
559 pupa (a), 24h sugar-fed (b), 24h blood-fed (c).

560 **Fig. 4: Volcano plot of differentially abundant miRNAs in CA-CC.** (A) Differentially
561 abundant miRNAs in CA-CC of pupae and sugar-fed adult female, (B) differentially abundant
562 miRNAs in CA-CC of sugar-fed and blood-fed adult females. miRNAs passing the criteria of
563 significantly differentially expressed ($p \leq 0.05$ and $FC \geq 2$) are labeled red, and those that did not
564 significantly change are shown in blue. Numbers in parentheses show the amount of
565 differentially expressed miRNAs between the two developmental stages. For the detailed list of
566 the differentially expressed miRNA see Table S2.

567 **Fig. 5: Hierarchical clustering analysis of differentially abundant miRNAs**. Hierarchical
568 clustering analysis of miRNAs expressed in the CA-CC of the three different developmental
569 stages revealed five major groups representing distinct expression patterns. miRNAs used for

clustering had a normalized average read count ≥ 200 in at least one of the developmental stages. Each point represents an average of three biological replicates.

Fig. 6: Validation of the RNA-Seq data using RT-qPCR. Comparison of expression of nine miRNAs that were abundant and differentially expressed among the three libraries. Black filled bars represent the number of transcripts detected by RT-qPCR, and normalized using the expression of the *U6* gene (U6 small nuclear RNA) (Left-Y axis). RT-qPCRs were performed with RNA extracted from three biological replicates of pools of 30 CA-CC dissected from pupae, sugar (sugar-fed adults) and blood (blood-fed adults) female mosquitoes. Empty bars represent the read counts from the sequenced libraries normalized as reads per million (Right-Y axis). Name of each miRNA analyzed is on top of each graph. Different letters above the columns indicate significant differences when the values for a particular developmental stage were compared within each dataset (one-way ANOVA $p < 0.05$, with Tukey's test of multiple comparisons).

583 **Supplementary data**
584
585 **Table S1: List of all the miRNAs detected in *Ae. aegypti* small RNA libraries**. In total, we
586 annotated 121 pre-miRNAs, with 101 of them already present in miRBase and 20 novel or
587 already reported in previous studies. These pre-miRNAs produced 234 mature miRNAs, with
588 196 already described in miRBase and 38 novel. After excluding duplicated mature miRNAs,
589 205 were unique.
590
591 **Table S2a: List of differentially expressed mRNAs between -24h female pupa and 24h**
592 **sugar-fed adult.** The miRNAs listed in this table are considered as differentially expressed in
593 CA-CC complex between -24h female pupa and 24h sugar-fed adult female (FDR $\geq$ 0.05 and FC
594 $\geq$ 2); FC – fold change, RC – read count, R – biological replicate, FDR - false discovery rate.
595
596 **Table S2b: List of differentially expressed mRNAs between 24h sugar-fed and 24h blood-**
597 **fed female adult.** The miRNAs listed in this table are considered as differentially expressed in
598 CA-CC complex between 24h sugar-fed adult and 24h blood-fed female adult (FDR $\geq$ 0.05 and
599 FC $\geq$ 2); FC – fold change, RC – read count, R – biological replicate, FDR - false discovery rate.
600
601 **Table S3: List of potential miRNA binding sites in the genes encoding JH biosynthetic**
602 **enzymes and CC peptides.** Three different algorithms were used to predict potential miRNA
603 binding sites in the thirteen *Ae. aegypti* genes encoding JH biosynthetic enzymes, as well as in
604 four genes encoding neuropeptides synthesized in the CC.
605
606 **Table S4: List of sequences of all primers used for RT-qPCR validation of miRNA**
607 **expression in this study.**
608
609 **Fig. S1: Hierarchical clustering analysis of all miRNAs expressed in the CA-CC of the**
610 **three different developmental stages**. Biological replicates of the same developmental stage
611 cluster together.
612
613 **Fig. S2: Prediction of miRNA targets in CA-CC using *in silico* tools.** Diagrams represent
614 Eukaryotic Clusters of Orthologous Groups (KOG) functional assignments for the 1323 high
615 confidence target mRNAs from the genome of *Ae. aegypti* (internal circles), from which 1215
616 are expressed in CA-CC complexes (external circles). Only mRNAs from Genbank with fully
617 annotated 5' and 3' UTR were subject of the target prediction.

Table 1. Small RNA read summary in *corpora allata-corpora cardiaca* libraries.

Sample ID	Number of reads	Percentage trimmed	Number of clean reads	Mapped to the genome	Total small RNA (UR)*	Total small RNA (RC)**	aae-miRNA (UR)	aae-miRNA (RC)	Detected aae-miRNA
Pupa_CA-1	38,101,222	74.66%	28,447,958	94.48%	202,841	26,491,384	4,315	6,468,995	147
Pupa_CA-2	23,956,132	42.20%	10,109,493	96.83%	80,463	9,275,342	2,123	1,741,917	130
Pupa_CA-3	25,660,874	57.02%	14,631,002	97.89%	83,098	13,782,327	2,536	2,174,602	140
Adult_CA-1	25,399,212	72.22%	18,343,474	91.35%	104,035	17,074,996	2,521	3,430,040	129
Adult_CA-2	24,082,807	55.43%	13,349,818	97.49%	46,905	12,791,939	1,596	1,128,345	126
Adult_CA-3	25,430,189	73.25%	18,626,804	98.12%	58,904	17,947,785	1,658	1,239,332	120
Blood_Fed_CA-1	23,826,661	79.81%	19,016,778	97.14%	74,246	18,181,492	1,703	1,066,477	124
Blood_Fed_CA-2	21,492,377	59.51%	12,790,236	96.29%	52,962	12,051,831	1,678	949,448	122
Blood_Fed_CA-3	24,127,060	57.26%	13,816,047	97.58%	53,096	13,170,699	1,553	958,663	117

* UR: Unique read sequence
** RC: Read count

-24h Pupa
No JH

24h Sugar-fed Adult
High JH

24h Blood-fed Adult
Low JH

Dissection of CA-CC (3 × n=50)

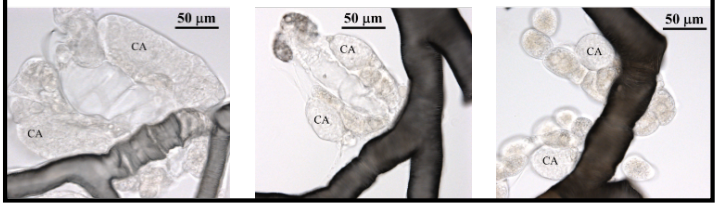

Total RNA extraction and generation of 9 small RNA libraries (Materials and Methods)

Data processing and data quality assessment (Table 1)

Revision *of* *Ae. aegypti* miRNA annotation (Table S1)

miRNA profiling of individual libraries and data normalization (GEO: GSE99498, Figure S1)

Determination of differential abundance of miRNAs among the three developmental stages (Figure 2, 3, S2, Table S2a, b)

Hierarchical clustering analysis of the miRNAs (Figure 4)

miRNA target prediction in CC-CA (Figure S3, Table S3)

Validation of miRNA differential expression (Figure 5)

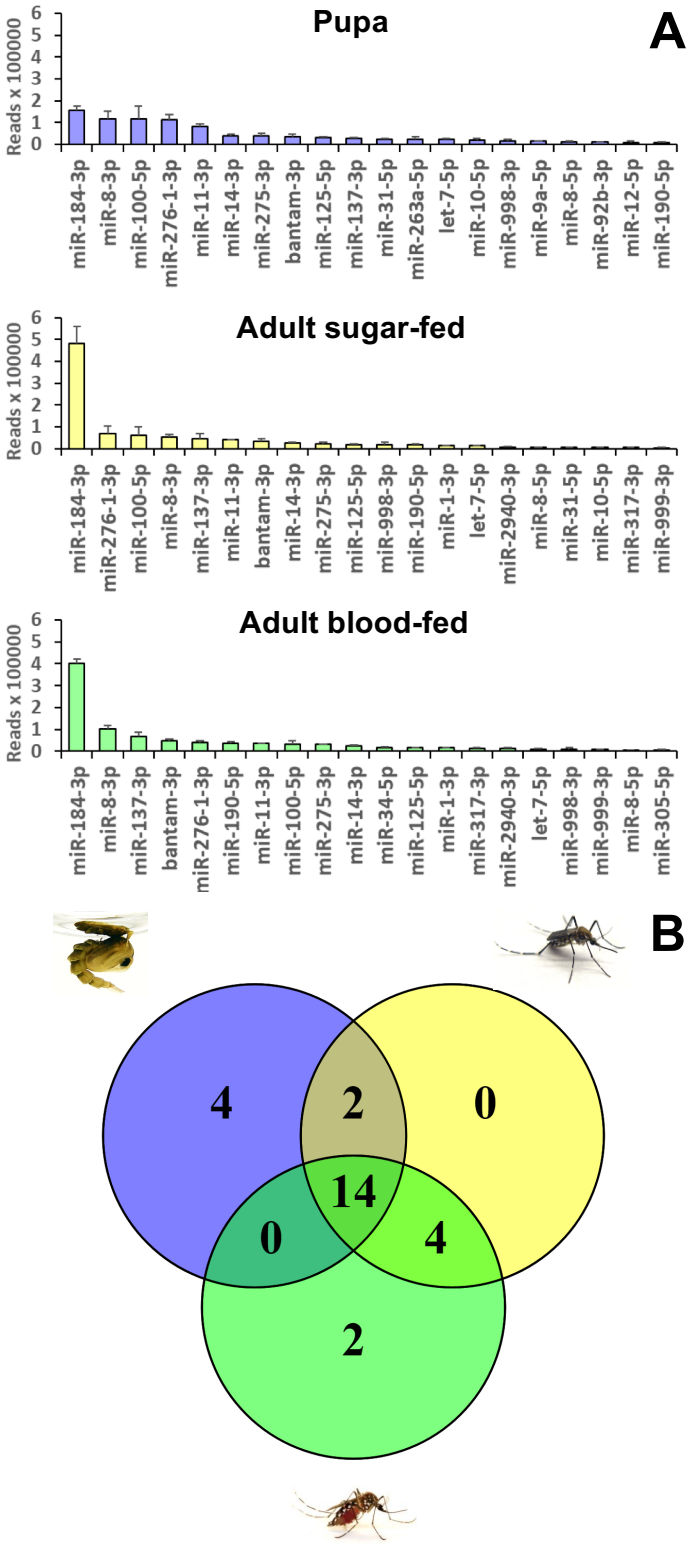
A
Pupa
Reads x 100000
0
1
2
3
4
5
6
miR-184-3p
miR-8-3p
miR-100-5p
miR-276-1-3p
miR-11-3p
miR-14-3p
miR-275-3p
bantam-3p
miR-125-5p
miR-137-3p
miR-31-5p
miR-263a-5p
let-7-5p
miR-10-5p
miR-998-3p
miR-9a-5p
miR-8-5p
miR-92b-3p
miR-12-5p
miR-190-5p
Adult sugar-fed
Reads x 100000
miR-184-3p
miR-276-1-3p
miR-100-5p
miR-8-3p
miR-137-3p
miR-11-3p
bantam-3p
miR-14-3p
miR-275-3p
miR-125-5p
miR-998-3p
miR-190-5p
miR-1-3p
let-7-5p
miR-2940-3p
miR-8-5p
miR-31-5p
miR-10-5p
miR-317-3p
miR-999-3p
Adult blood-fed
Reads x 100000
miR-184-3p
miR-8-3p
miR-137-3p
bantam-3p
miR-276-1-3p
miR-190-5p
miR-11-3p
miR-100-5p
miR-275-3p
miR-14-3p
miR-34-5p
miR-125-5p
miR-1-3p
miR-317-3p
miR-2940-3p
let-7-5p
miR-998-3p
miR-999-3p
miR-8-5p
miR-305-5p
B
4
2
0
14
0
4
2

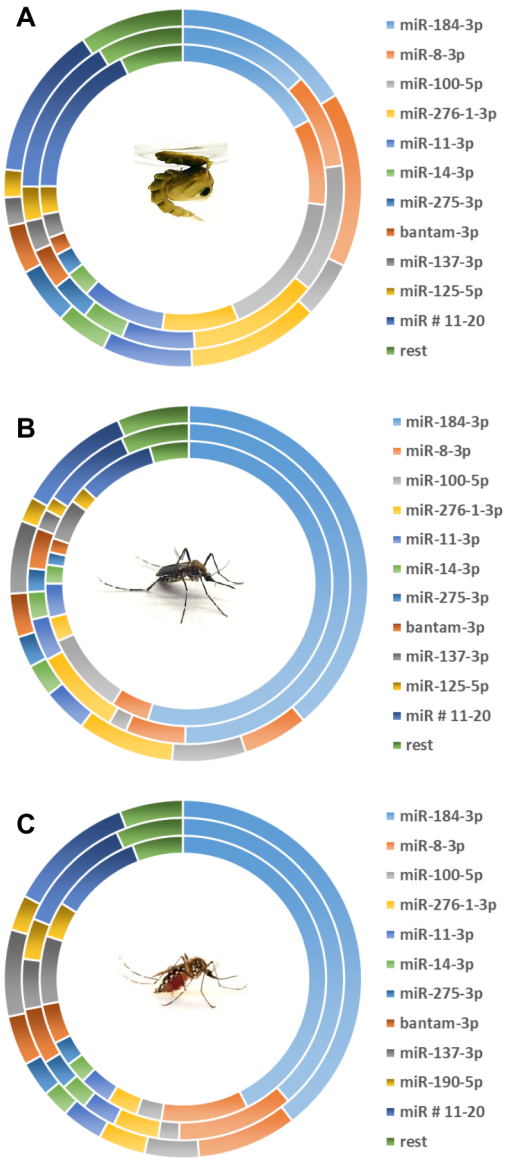

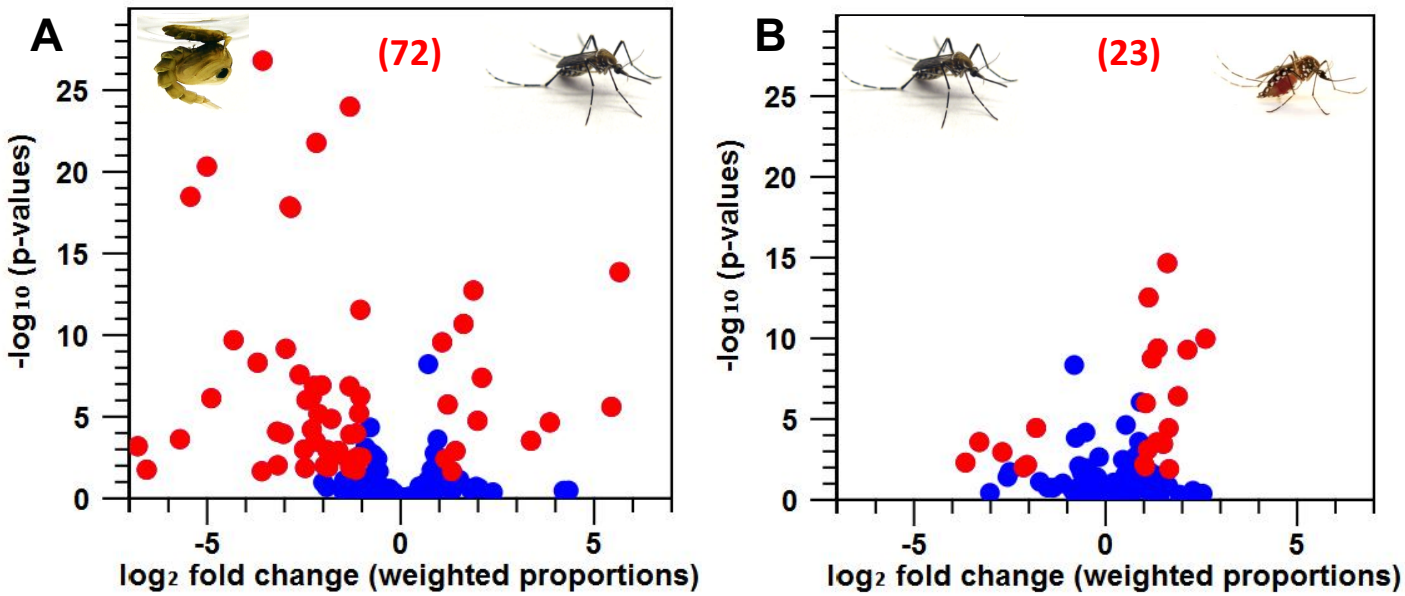
A
(72)
-log10 (p-values)
25
20
15
10
5
0
-5
0
5
log2 fold change (weighted proportions)
B
(23)
-log10 (p-values)
25
20
15
10
5
0
-5
0
5
log2 fold change (weighted proportions)

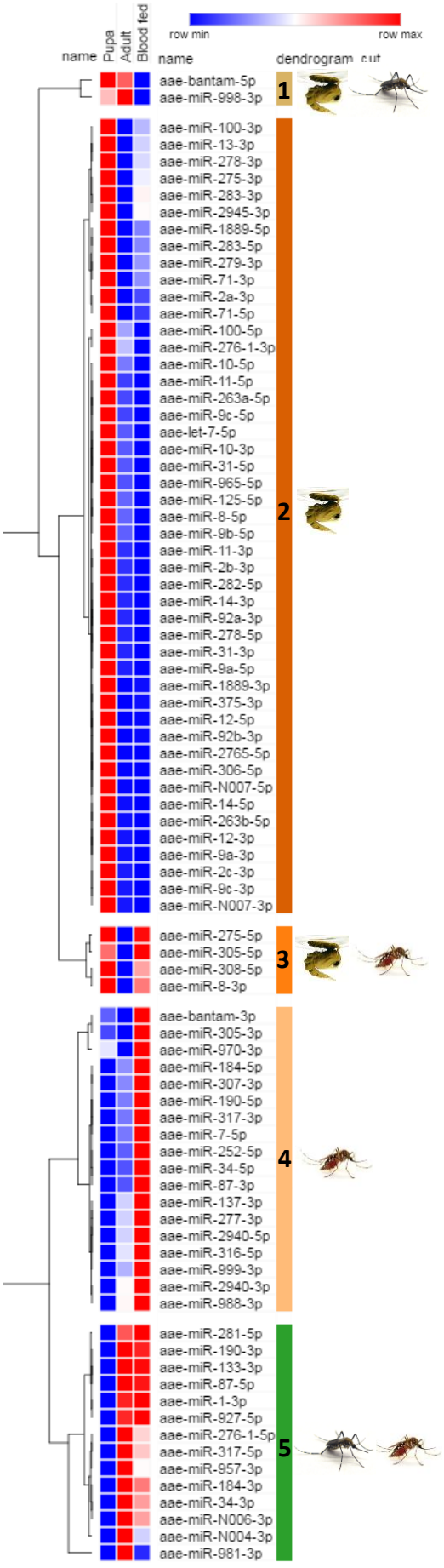
row min
row max
name
Pupa
Adult
Blood fed
name
dendrogram cut
aae-bantam-5p
aae-miR-998-3p
1
aae-miR-100-3p
aae-miR-13-3p
aae-miR-278-3p
aae-miR-275-3p
aae-miR-283-3p
aae-miR-2945-3p
aae-miR-1889-5p
aae-miR-283-5p
aae-miR-279-3p
aae-miR-71-3p
aae-miR-2a-3p
aae-miR-71-5p
aae-miR-100-5p
aae-miR-276-1-3p
aae-miR-10-5p
aae-miR-11-5p
aae-miR-263a-5p
aae-miR-9c-5p
aae-let-7-5p
aae-miR-10-3p
aae-miR-31-5p
aae-miR-965-5p
aae-miR-125-5p
aae-miR-8-5p
aae-miR-9b-5p
aae-miR-11-3p
aae-miR-2b-3p
aae-miR-282-5p
aae-miR-14-3p
aae-miR-92a-3p
aae-miR-278-5p
aae-miR-31-3p
aae-miR-9a-5p
aae-miR-1889-3p
aae-miR-375-3p
aae-miR-12-5p
aae-miR-92b-3p
aae-miR-2765-5p
aae-miR-306-5p
aae-miR-N007-5p
aae-miR-14-5p
aae-miR-263b-5p
aae-miR-12-3p
aae-miR-9a-3p
aae-miR-2c-3p
aae-miR-9c-3p
aae-miR-N007-3p
2
aae-miR-275-5p
aae-miR-305-5p
aae-miR-308-5p
aae-miR-8-3p
3
aae-bantam-3p
aae-miR-305-3p
aae-miR-970-3p
aae-miR-184-5p
aae-miR-307-3p
aae-miR-190-5p
aae-miR-317-3p
aae-miR-7-5p
aae-miR-252-5p
aae-miR-34-5p
aae-miR-87-3p
aae-miR-137-3p
aae-miR-277-3p
aae-miR-2940-5p
aae-miR-316-5p
aae-miR-999-3p
aae-miR-2940-3p
aae-miR-988-3p
4
aae-miR-281-5p
aae-miR-190-3p
aae-miR-133-3p
aae-miR-87-5p
aae-miR-1-3p
aae-miR-927-5p
aae-miR-276-1-5p
aae-miR-317-5p
aae-miR-957-3p
aae-miR-184-3p
aae-miR-34-3p
aae-miR-N006-3p
aae-miR-N004-3p
aae-miR-981-3p
5

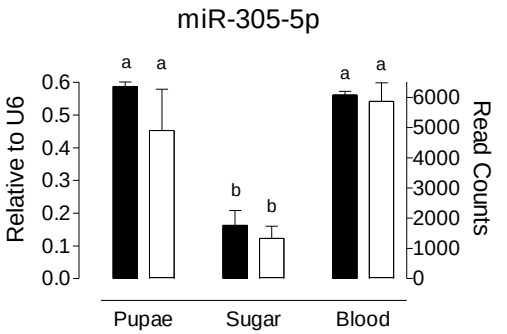

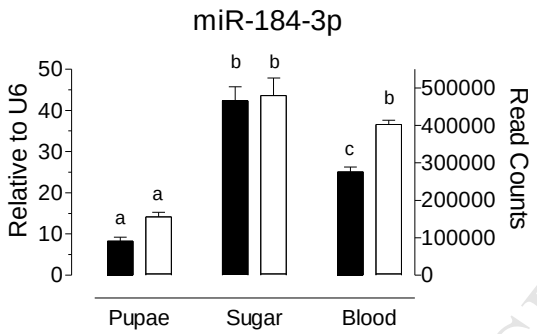

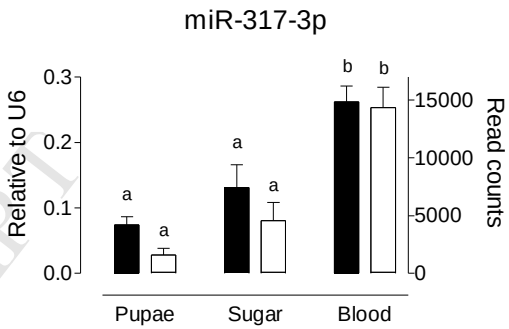

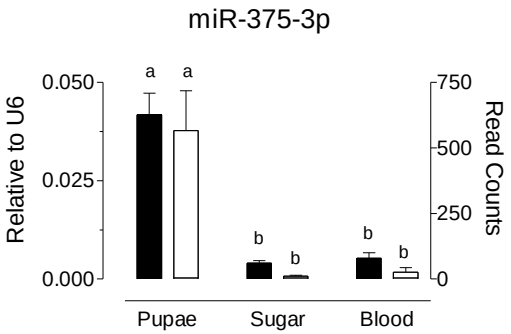

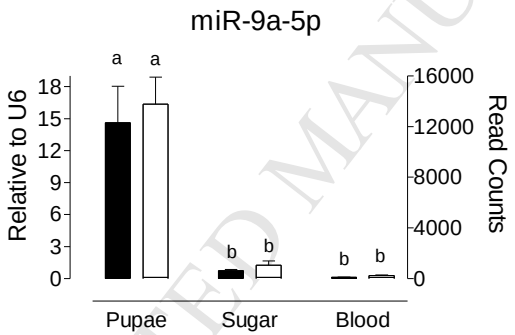

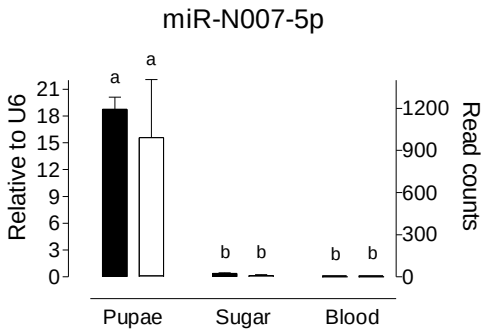

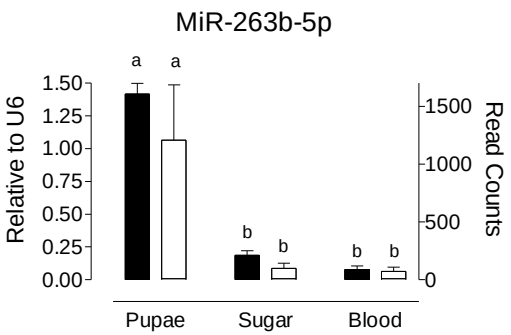

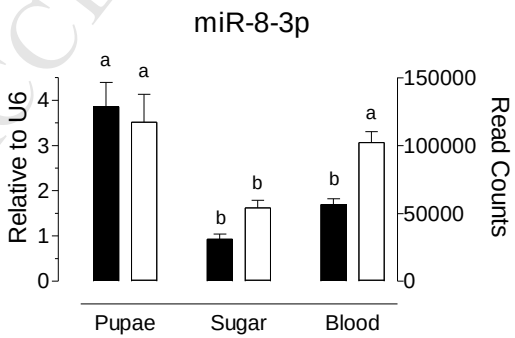

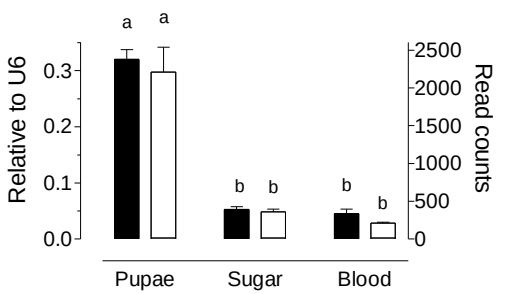

Highlights

- microRNA profiles of corpora allata and cardiaca in three distinct developmental stages of *Aedes aegypti* mosquitoes were compared
- Significant alterations of 84 microRNAs were found, in particular between the pupal and adult stages
- A number of microRNAs were found to potentially target juvenile hormone biosynthetic enzymes
- Gene ontology analysis of target genes of microRNAs revealed their involvement in various biological processes